

A Medical Decision Support System for Explainable Multimodal Detection of Non-Small Cell Lung Cancer Using Clinical and PET Data

Nikolaos I. Papandrianos, Anna A. Feleki, Ioannis D. Apostolopoulos, Elpiniki I. Papageorgiou
 Department of Energy Systems, University of Thessaly,
 Gaiopolis Campus, 41500
 Larissa, Greece
 npapandrianos@uth.gr, annafele1@uth.gr,
elpinikipapageorgiou@uth.gr

Jose Maria Alonso Moral
 Centro Singular de Investigación en Tecnoloxías
 Intelixentes (CiTIUS), Universidade de Santiago de
 Compostella, 15782,
 Santiago de Compostela, Spain
josemaria.alonso.moral@usc.es

Nikolaos D. Papathanasiou, Dimitrios J. Apostolopoulos
 Department of Nuclear Medicine, University General
 Hospital of Patras, University of Patras, 265-00
 Patras, Greece
nikopapath@upatras.gr, dimap@upatras.gr

Javier Andreu-Perez
 Centre for Computational Intelligence, School of Computer
 Science and Electronic Engineering, University of Essex,
 Colchester, United Kingdom
j.andreu-perez@essex.ac.uk

Abstract— Non-small cell lung cancer is a prevalent form of lung cancer, with Solitary Pulmonary Nodules (SPNs) as a key indicator. Early detection and accurate diagnosis are critical for effective treatment. While Convolutional Neural Networks (CNNs) have been successful in diagnosing SPNs from Computed Tomography (CT) and Positron Emission Tomography (PET) imaging, they lack explainability. To address this, we applied DeepFCM, a multimodal approach that combines Fuzzy Cognitive Maps (FCMs) with CNNs, integrating clinical and PET imaging data to predict SPN malignancy. Clinical data include patient characteristics (i.e., gender, age, Body Mass Index, Glucose Levels) and SPN characteristics (diameter, Standardized Uptake Value (SUV)max, location, type, and margins). Predictions from the RGB-CNN, trained on PET images, are used as additional inputs for DeepFCM. Initially defined by nuclear experts using fuzzy sets, concept interconnections were adapted with Particle Swarm Optimization (PSO) and Genetic Algorithm (GA). DeepFCM is integrated into a Medical Decision Support System (MDSS) to enable data-driven predictions for NSCLC. To improve explainability, Gradient-weighted Class Activation Mapping (Grad-CAM) highlights significant image regions, while DeepFCM illustrates the relationships between each feature to NSCLC diagnosis. Natural Language Generation (NLG) is applied to explain the DeepFCM decision-making process by demonstrating each feature's impact on the diagnosis in human-understandable language. (*Abstract*)

Keywords—Fuzzy Cognitive Maps; Non-small Cell Lung Cancer; Particle Swarm Optimization; Genetic Algorithm.

I. INTRODUCTION

Non-Small Cell Lung Cancer (NSCLC) constitutes approximately 85% of all lung cancer cases globally [1].

NSCLC can often be presented as a Solitary Pulmonary Nodule (SPN) on imaging studies, necessitating further evaluation to determine if the nodule is benign or malignant, which presents challenges. Most individuals with early-stage lung cancer do not exhibit typical symptoms. However, once symptoms like cough and hemoptysis appear, many patients have already progressed to the middle or late stages of lung cancer, with metastasis occurring in some cases [2]. Deep Learning (DL) methodologies like CNN have been applied and published to detect SPN malignancies. In [3], the authors proposed an ensemble-based prediction model for NSCLC recurrence following surgical resection. The method integrated three neural network models, each trained separately on clinical data, handcrafted radiomic (HCR) features, and deep learning radiomic (DLR) features derived from CT images. The outputs of these models were combined using an ensemble analyzer to make the final prediction. Data from two institutions were utilized, involving standardized Computed Tomography (CT) images and relevant clinical features, excluding incomplete cases. The proposed ensemble model demonstrated superior accuracy using only single data types, achieving an 11.69% higher accuracy than the staging baseline. In [4], the VGG19 model was applied to classify CT and Positron Emission Tomography (PET) images, using the extracted features from VGG19 for further analysis. These outputs, along with additional SPN characteristics, were fed into an XGBoost model, which conducted the final diagnosis by merging imaging data and clinical features to enhance diagnostic precision. 402 patient cases were used with human annotations for internal validation and 96 histopathologically confirmed cases for external evaluation. The model achieved a 97% agreement with human experts and showed 85%

diagnostic accuracy on the external dataset. The most important predictors identified in this study were the Standardized Uptake Value (SUV)_{max} value and the nodule diameter. Additionally, in [5], the authors explored multimodal learning on the «CoLIaborative multi-sources Radiopathomics approach for personalized Oncology in non-small cell lung cancer» (CLARO) dataset for NSCLC, combining clinical data and imaging from a patient cohort to predict overall survival. A late fusion ensemble approach optimally integrated classifiers from different modalities, including a ResNet34 and a VGG11-BN for the imaging modality and a TABNET for the clinical modality, by solving a multiobjective optimization problem to maximize performance and diversity. Results indicate the proposed multimodal ensemble outperforms unimodal models, achieving 75% accuracy, 77.7% F1-score, and 84% recall. Furthermore, in [6], a two-stage multimodal learning framework was developed for diagnosing pulmonary nodules in PET/CT images. Pulmonary parenchyma segmentation was applied in the first stage with a pre-trained U-Net model. The second stage focused on extracting image-level and feature-level characteristics by utilizing a 3D Inception-Residual Net (ResNet) with a convolutional block attention module and a dense-voting fusion mechanism. The model's performance was validated on real clinical data, achieving mean scores of 89.98% accuracy, 89.21% precision, 84.75% recall, 93.38% specificity, 86.83% F1 score, and 0.9227 area under the curve (AUC). In [7], a stacked 3D CNN model was implemented to classify SPN in PET/CT images. 113 participants were included. Data augmentation was applied to increase the size of the training dataset, with random rotation, and by applying Gaussian noise, to differentiate the augmented images. Grad-CAM was applied as a post-hoc explainability technique to get insights from the CNN model. The 3D CNN attained a sensibility of 80.00%, a specificity of 69.23%, and an accuracy of 73.91%. Four-fold cross-validation was performed as an evaluation method.

In a preliminary previous work [8], DeepFCM was implemented in the context of a research-funded project named EMERALD [9] for the diagnosis of NSCLC assessing PET images with the diameter of the SPN and SUV_{max} variable as two only clinical features. RGB-CNN was constructed from scratch, and trained on PET images, where the CNN predictions for each image instance were included as an additional input concept. The FCM-weight analysis revealed the interconnections between various concepts, illustrating how they influence each other. In addition, DeepFCM was employed for the effective diagnosis of Coronary Artery Disease (CAD) with Polar map images, along with clinical and demographic information about the patients presenting the FCM-weighted analysis of concepts [10] and in [11], where the results were enhanced with the incorporation of visual (Grad-CAM) and textual (supported by language models) explanations. This way, we go a step ahead from eXplainable Artificial Intelligence (XAI) methodologies towards Trustworthy AI [12].

This study aims to develop DeepFCM with the following set of clinical features, which include patient demographic information like gender, age, Body Mass Index (BMI),

Glucose Level (GLU) value, and definite parameters such as SPN location, type, and margins, along with PET image data for NSCLC diagnosis. Robust XAI techniques are employed to facilitate understanding of the model, including Grad-CAM, which explains the decision-making process of CNN results. Moreover, Natural Language Generation (NLG) techniques translate DeepFCM outputs into human-readable linguistic pieces of information, further enhancing the overall clarity and transparency of the model's predictions.

The remainder of the paper is organized as follows: Section II presents the methods and methodology, including an overview of the patient data and the DeepFCM approach. Section III details the research results, while Section IV provides the concluding remarks.

II. MATERIAL AND METHODS

This section details the data acquisition process for PET data, followed by the steps of the proposed DeepFCM methodology.

A. Patient Data

The PET/CT image data was recorded in the Clinical Sector of the Department of Nuclear Medicine at the University Hospital of Patras using a hybrid PET/CT scanner (Discovery iQ3 s116, General Electric Healthcare). This system uses three detector rings with a 15cm field of view to reconstruct 35 axial images at 4.25mm intervals. 3D volumes are acquired to represent the whole body using various bed positions. At the same time, the patient was in a supine position. Two experienced human readers (N.P., 10 years of experience, D.J.A., 30 years of experience) characterized the SPN malignancy with patient follow-up. The study's nature waives the requirement for obtaining patients' informed consent. From 2020 to 2023, more than 800 PET/CT scans were reviewed to identify potential participants. Patients without detected SPNs or with SPNs with a diameter greater than 30mm were excluded. 456 patients with a single SPN were qualified. The total benign cases were 222 and the total malignant cases were 234. Experts annotated CT scan slices, noting the finding's type, location, margins, diameter, and SUV_{max} and SPN diameter along with demographic information about each patient (gender, age, BMI). The SUV_{max} and diameter parameters were extracted from the PET scan. Each SPN finding is represented by a single 2D slice in which the full extent of the nodule is visible.

B. Deep Fuzzy Cognitive Map

In this research paper, we demonstrate the capabilities of our MDSS, specifically highlighting the DeepFCM method for diagnosing NSCLC using PET images alongside the clinical characteristics. The FCM-based model processed the values as input concepts, leveraging FCM's ability to convert input knowledge into system concepts with established causal relationships among them [13]. Expert knowledge is provided in the form of fuzzy sets with linguistic values defining the input-output interconnections among concepts. The linguistic values are transformed into numerical values to be utilized in the algorithm [14]. As interpretability techniques, Grad-CAM was employed to interpret CNN

predictions, while NLG was used to translate the DeepFCM outputs into human-readable explanations. Figure 1 presents the full methodological framework of the DeepFCM approach used in this study, detailing both the training process and the inference mechanism within the MDSS functionality. Following, the steps of the DeepFCM methodological process are analyzed.

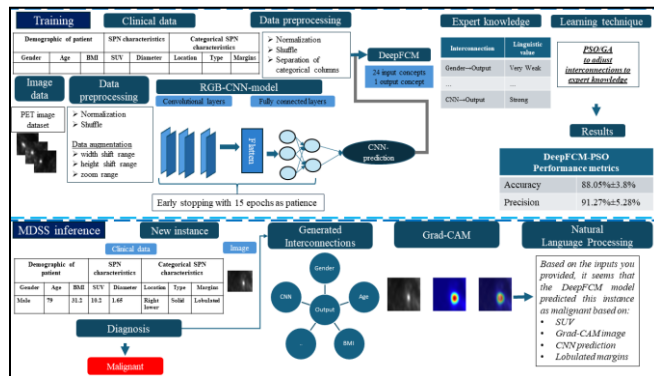


Figure 1. DeepFCM Methodological Pipeline Framework for NSCLC Diagnosis Using Clinical Data and PET Imaging Data

The clinical data includes patient demographic information about the patient such as gender, age, and BMI, GLU, as well as characteristics of the SPN such as SUVmax value, nodule diameter, and three SPN categorical variables type, location, and margins each segmented by their respective values.

First, age was preprocessed with the Min-Max normalization technique [15] and the variables BMI, GLU, SUV, and diameter were divided with their maximum value of 70, 192, 30, and 3 accordingly to be rescaled into the spectrum [0,1]. The SPN categorical variables, including location, type, and margins, were separated into individual columns, with one-hot encoding process. The separated columns generated from categorical variables with SPN characteristics along with the demographic of the patient result in a total of twenty-three clinical characteristics. RGB-CNN was constructed from scratch and trained with the PET dataset; being able to extract a prediction for each image instance. The RGB-CNN predictions were incorporated as an additional input concept alongside clinical data, collectively forming twenty-four distinct input concepts for the DeepFCM model. This model leverages both clinical values and CNN-derived predictions, integrating them into a cohesive framework that enhances interpretability and insight into the diagnostic process. By incorporating clinical and imaging data, DeepFCM generates results that are not only accurate but also transparent, enabling a clear understanding of how each concept impacts the final diagnosis. Through CNN’s robust feature extraction from imaging data, combined with the FCM’s transparent framework for mapping interconnections, DeepFCM delivers an insightful diagnostic tool that provides clinicians with a nuanced view of the decision-making process. This combined approach strengthens the system’s capacity to guide decisions, making DeepFCM a comprehensive and

interpretable tool in the context of medical diagnostics [11]. A 10-fold cross-validation approach was implemented to ensure the generalizability of results by partitioning the dataset into 10 batches, where each batch served as the testing fold while the remaining nine served as the training folds [16].

In this study, Particle Swarm Optimization (PSO), and Genetic Algorithm (GA) were incorporated into the DeepFCM learning process to adjust the interconnections among concepts and thus be in line with the provided expert knowledge. PSO [17] is a population-based approach with particles exploring the search space. PSO can be integrated into the FCM learning process by treating the interconnections (weights) between concepts as particles in the search space. Each particle (weight) adjusts its position based on its own best-known position and the best-known positions of its neighbors, iteratively optimizing the FCM weight matrix to minimize the error between predicted and actual outcomes. GA integrates with FCM learning by encoding the weights between concepts as chromosomes, which evolve over multiple generations. Through selection, crossover, and mutation, GA searches for the optimal weight matrix that best aligns with expert knowledge, improving the predictive power of the FCM model [18]. Both optimization methods calculate the weights (interconnections) among DeepFCM concepts to improve classification performance. Even though they perform similarly in the benchmark classification metrics, the GA applied for DeepFCM learning emerges with lower computational latency.

Overall, the learning process creates a weight matrix to minimize the error function, used by DeepFCM for NSCLC diagnosis. For each case, DeepFCM uses the selected weight matrix to provide a diagnosis and at the same time to visualize the input-output relationships, enhancing transparency in the decision-making process.

Regarding XAI techniques, Grad-CAM is used to interpret RGB-CNN predictions, by highlighting the most influential regions that signify the prediction. Grad-CAM implemented by Selvaraju [19] leverages the feature maps produced by the final convolutional layer of the CNN to identify the most relevant regions in the image that contribute to the model’s prediction. By computing the gradients of the target class concerning these feature maps, Grad-CAM generates a heatmap that highlights the areas of the image most influential in the decision-making process, providing visual insights into the model’s focus [19]. In addition, textual explanations were generated with GPT-4, a pre-trained large language model, which has an Application Programming Interface (API) provided by OpenAI [20], as an NLG technique. Namely, a prompt is provided to GPT-4, containing the user-inputted variable values, the DeepFCM result, the CNN prediction, and the corresponding DeepFCM weight values, along with instructions about how to realize the structure of the requested textual explanation. This enables GPT-4 to generate a comprehensive natural explanation of the decision-making process, offering clear insights into how DeepFCM arrived at its diagnosis.

III. RESULTS

This section presents the classification results along with the included XAI techniques, with the DeepFCM, generated interconnections, heatmap image, and NLG reasoning, to interpret the DeepFCM decision-making process. Additionally, it demonstrates the functionality of MDSS in classifying NSCLC diagnoses using PET and clinical data.

A. Classification Results

For classifying NSCLC data into two categories, benign and malignant, CNN models and DeepFCM were applied and compared with the literature state of the art for similar cases. Table I provides a summary of the performance metrics across different investigated models. Initially, the results of the RGB-CNN model, which was trained exclusively on PET image data are presented. Next, DeepFCM results are illustrated, following the proposed multimodal approach integrating clinical and imaging data (see section above), optimized using PSO and GA. Finally, the proposed models are compared against state-of-the-art models cited in the literature review [3]-[5]. Mean values and standard deviations illustrate the consistency of results for each model. Additionally, confidence intervals (CIs) are provided for the second to last model, offering insight into the precision and reliability of its performance estimates.

TABLE I. DEMONSTRATION OF RESULTS

Accuracy	Loss	Sensitivity	Specificity	Precision
RGB-CNN model				
83.12%±6.43%	0.3	92.26±6.18%	91.91±9.21%	91.31±5.75%
Proposed study (DeepFCM-PSO and DeepFCM-GA)				
88.14%±3.8%	0.12	88.36±5.23%	87.29±7.48%	91.27±5.28%
87.08%±5.96%	0.13	84.56±12.29%	85.38±6.83%	87.79±6.16%
Literature study [3]				
73.23%±6.0%	-	80.08±6.4%	-	75.71±4.8%
Literature study [4]				
85.21 (95% CI: 83.74–86.68)		81.23 (95% CI: 79.22–83.24)	95.37 (95% CI: 92.99–97.75)	
Literature study [5]				
75%±16.2%	-	84%±15.17%	-	-

In particular, RGB-CNN achieved 83.12% accuracy, while DeepFCM's multimodal approach improved the classification accuracy, with PSO reaching 88.14% and GA 87.08%. Incorporating additional clinical information, the overall performance has been enhanced. DeepFCM models showed smaller deviations in the calculated metrics, indicating consistency. State-of-the-art multimodal approaches attained 73.23% [3], 85.21% [4], and 75% [5] accuracy, highlighting the improvements achieved by the proposed model.

B. MDSS illustrative example

We present the DeepFCM results through MDSS for NSCLC diagnosis using the DeepFCM-PSO model, which achieved the best metrics. The DeepFCM graph demonstrates the interconnections among concepts, Grad-CAM provides visual CNN explanations, while GPT-4 translates outputs into clear, understandable interpretations.

1) MDSS Diagnosis

Figure 2 showcases the DeepFCM diagnosis along with the generated DeepFCM graph, illustrating the interconnections between concepts. The patient refers to a 63-year-old male patient with a BMI of 27.8, a GLU value of 89, an SUVmax of 10.2, and an SPN diameter of 2.7 cm located in the right lower lobe. The type of SPN is semi-solid with lobulated margins.

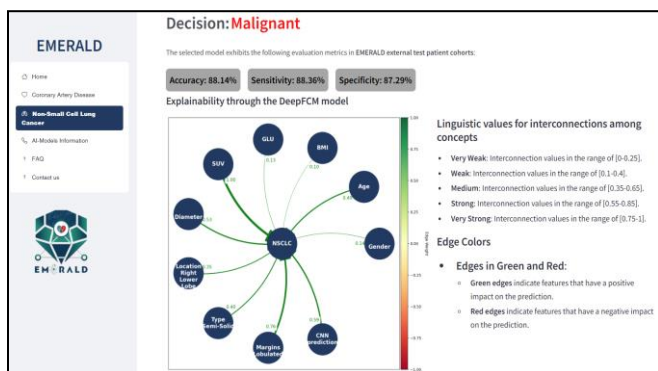


Figure 2. MDSS screenshot: Illustrative example with DeepFCM-PSO Integration for NSCLC Diagnosis Using PET Imaging and Clinical Data.

2) Grad-CAM

Figure 3 showcases the Grad-CAM application through MDSS, with JET colormap to highlight impactful regions in red and less impactful ones in blue. The figure includes the cropped ROI image, the heatmap indicating key areas, and the overlay combining both. The CNN accurately classified the malignant lesion, and Grad-CAM effectively localized and highlighted in red the malignant SPN region, providing visual justification for the RGB-CNN model's prediction of malignancy.

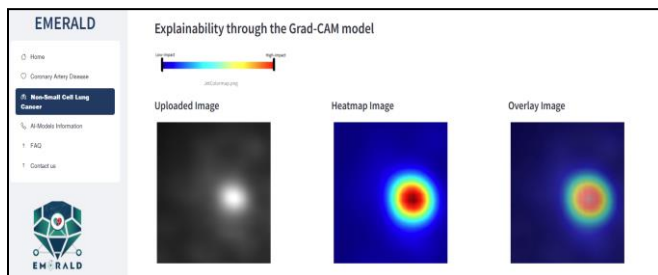


Figure 3. Grad-CAM Application Integrated into MDSS as an XAI Technique for PET Image Analysis.

3) Textual explanations

In Figure 4, we present the results from the GPT-based textual explainer integrated within the MDSS, which offers a

clear and detailed analysis of the clinical factors contributing to the malignancy prediction. A prompt was carefully constructed, incorporating several key components: the CNN and DeepFCM predictions, the input clinical values, the heatmap image generated through Grad-CAM, and the DeepFCM-generated interconnections. This combination allows the explainer to highlight the most influential factors, while seamlessly integrating image analysis and model predictions.

DeepFCM has accurately classified the SPN as malignant, supported by both clinical and imaging data. Key clinical factors such as high SUV (10.2), significant nodule diameter (2.7 cm), and lobulated margins play pivotal roles in this diagnosis. Additionally, the image analysis, including the original scan and Grad-CAM heatmap, reinforces the malignancy prediction by highlighting critical regions associated with increased metabolic activity and irregular growth patterns. The integration of clinical insights, CNN predictions, and visual heatmap evidence provides a comprehensive and explainable diagnosis for the nuclear doctor, ensuring consistency and clarity in the interpretation of the results.

IV. CONCLUSIONS

DeepFCM’s capabilities establish it as a fundamental tool for achieving accurate SPN diagnoses in PET images and clinical data while providing explainability of results, enhancing DeepFCM’s suitability to be incorporated into doctors’ diagnosis process. DeepFCM stands out as a transparent tool for effective NSCLC diagnosis by incorporating explainable methodologies.

DeepFCM’s interconnections between clinical and imaging data, using PSO and GA, highlight key features like SUV, nodule diameter, and the SPN type. This alignment validates its accuracy in prioritizing factors influencing NSCLC malignancy. Its ability to reveal meaningful clinical-imaging connections solidifies its potential as a reliable diagnostic tool, aiding clinicians in identifying critical factors for accurate NSCLC diagnosis.

Explanation through NLG reasoning

Conclusions:

The Deep Fuzzy Cognitive Map (DeepFCM) has concluded that the Solitary Pulmonary Nodule (SPN) in this case is malignant. This aligns with the Convolutional Neural Network (CNN) model's decision, which also indicated malignancy. The clinical values and image analyses collectively support this decision, with significant influence from specific clinical features and image regions.

Further Details:

- **Clinical Values:**
 - **Standardized Uptake Value (SUV):** This is the most significant clinical factor, with a very high influence on the outcome. The SUV of 10.2 is substantially elevated, indicating high metabolic activity typical of malignant nodules.
 - **Diameter:** The nodule's diameter of 2.7 cm is another critical factor, as larger nodules have a higher probability of being malignant.
 - **Margins (Lobulated):** The lobulated margins are a strong indicator of malignancy, contributing significantly to the decision.
 - **Type (Semi-Solid):** Semi-solid nodules are more likely to be malignant compared to purely solid or purely ground-glass nodules.
 - **Location (Right Lower Lobe):** While the location has a moderate influence, nodules in the lower lobes are often scrutinized more closely in clinical practice.
- **Image Analysis:**
 - **Original Image:** The SPN's characteristics, such as its size and margins, are consistent with malignant features. The nodule's appearance in the original image suggests irregularity and potential invasiveness.
 - **Grad-CAM Heatmap:** The heatmap highlights areas of high importance in red, which correspond to the regions of the nodule with the most significant features indicating malignancy. These regions likely show increased metabolic activity or irregular growth patterns, supporting the malignant classification.

In summary, the combination of elevated SUV, significant nodule diameter, lobulated margins, and the semi-solid nature of the nodule, along with the supporting image analysis, strongly suggests malignancy. This case does not require further investigation as both the CNN model and DeepFCM are in agreement.

Figure 4. Explanation of DeepFCM Prediction for NSCLC Analysis Using NLG Reasoning.

This approach aligned with nuclear experts' assessments and helped non-specialists understand the model’s logic. Grad-CAM detected the SPN region in the PET image, which RGB-CNN classified as malignant. The heatmap highlighted key high metabolic activity areas within the nodule, visually explaining the model's decision. This validated the model’s focus on relevant regions, offering clinicians a clear understanding of CNN’s classification process, and enhancing transparency in diagnosis. The study has limitations, primarily due to the dataset being sourced from a single hospital, which affects its representativeness and generalizability across different regions and healthcare settings. This may limit the broader applicability of the findings. Further improvement could be achieved by incorporating diverse datasets to enhance model robustness and applicability.

MDSS incorporating DeepFCM is a valuable tool for accurate SPN diagnosis in PET images and clinical data. By providing clear, explainable results, MDSS enhances the diagnostic process, making it a vital asset in clinical settings. This system not only improves the accuracy of diagnoses but also ensures that the reasoning behind each diagnosis is transparent and understandable, fostering trust in AI-driven healthcare solutions.

DATA AVAILABILITY

The dataset used in this study is not publicly available due to hospital medical data privacy constraints. However, it can be provided by the corresponding author upon reasonable request. The source code is available in [21].

ACKNOWLEDGEMENT

The research project was supported by the Hellenic Foundation for Research and Innovation (H.F.R.I.) under the "2nd Call for H.F.R.I. Research Projects to support Faculty Members & Researchers" (Project Number: 3656).

REFERENCES

- [1] I. D. Apostolopoulos, D. J. Apostolopoulos, and G. S. Panayiotakis, "Solitary Pulmonary Nodule malignancy classification utilising 3D features and semi-supervised Deep Learning," in 2022 13th International Conference on Information, Intelligence, Systems & Applications (IISA), Jul. 2022, pp. 1–6. doi: 10.1109/IISA56318.2022.9904334.
- [2] E. Gershman, R. Guthrie, K. Swiatek, and S. Shojaee, "Management of hemoptysis in patients with lung cancer," *Annals of Translational Medicine*, vol. 7, no. 15, p. 358, Aug. 2019, doi: 10.21037/atm.2019.04.91.
- [3] G. Kim, S. Moon, and J.-H. Choi, "Deep Learning with Multimodal Integration for Predicting Recurrence in Patients with Non-Small Cell Lung Cancer," *Sensors (Basel)*, vol. 22, no. 17, p. 6594, Aug. 2022, doi: 10.3390/s22176594.
- [4] I. D. Apostolopoulos, N. D. Papathanasiou, D. J. Apostolopoulos, N. Papandrianos, and E. I. Papageorgiou, "A Multi-Modal Machine Learning Methodology for Predicting Solitary Pulmonary Nodule Malignancy in Patients Undergoing PET/CT Examination," *Big Data and Cognitive Computing*, vol. 8, no. 8, Art. no. 8, Aug. 2024, doi: 10.3390/bdcc8080085.
- [5] C. M. Caruso et al., "A Multimodal Ensemble Driven by Multiobjective Optimisation to Predict Overall Survival in

- Non-Small-Cell Lung Cancer,” *Journal of Imaging*, vol. 8, no. 11, Art. no. 11, Nov. 2022, doi: 10.3390/jimaging8110298.
- [6] T. Li et al., “Fully automated classification of pulmonary nodules in positron emission tomography-computed tomography imaging using a two-stage multimodal learning approach,” *Quant Imaging Med Surg*, vol. 14, no. 8, pp. 5526–5540, Aug. 2024, doi: 10.21037/qims-24-234.
- [7] V. M. Alves, J. dos Santos Cardoso, and J. Gama, “Classification of Pulmonary Nodules in 2-[18F]FDG PET/CT Images with a 3D Convolutional Neural Network,” *Nucl Med Mol Imaging*, vol. 58, no. 1, pp. 9–24, Feb. 2024, doi: 10.1007/s13139-023-00821-6.
- [8] A. Feleki et al., “Deep Fuzzy Cognitive Map methodology for Non-Small Cell Lung Cancer diagnosis based on Positron Emission Tomography imaging,” in *2023 14th International Conference on Information, Intelligence, Systems & Applications (IISA)*, Jul. 2023, pp. 1–6. doi: 10.1109/IISA59645.2023.10345912.
- [9] “HOME,” EMERALD. Accessed: Oct. 27, 2024. [Online]. Available: <https://emerald.uth.gr/>
- [10] A. Feleki, I. D. Apostolopoulos, K. Papageorgiou, E. I. Papageorgiou, D. J. Apostolopoulos, and N. I. Papandrianos, “A Fuzzy Cognitive Map Learning Approach for Coronary Artery Disease Diagnosis in Nuclear Medicine,” in *Fuzzy Logic and Technology, and Aggregation Operators: 13th Conference of the European Society for Fuzzy Logic and Technology, EUSFLAT 2023*, Jun. 2023, pp. 14–25. doi: 10.1007/978-3-031-39965-7_2.
- [11] A. Feleki et al., “Explainable Deep Fuzzy Cognitive Map Diagnosis of Coronary Artery Disease: Integrating Myocardial Perfusion Imaging, Clinical Data, and Natural Language Insights,” *Applied Sciences*, vol. 13, p. 11953, Nov. 2023, doi: 10.3390/app132111953.
- [12] S. Ali et al., “Explainable Artificial Intelligence (XAI): What we know and what is left to attain Trustworthy Artificial Intelligence,” *Inf. Fusion*, vol. 99, no. C, Nov. 2023, doi: 10.1016/j.inffus.2023.101805.
- [13] E. I. Papageorgiou, N. I. Papandrianos, D. Apostolopoulos, and P. Vassilakos, “Complementary use of Fuzzy Decision Trees and Augmented Fuzzy Cognitive Maps for Decision Making in Medical Informatics,” *2008 International Conference on BioMedical Engineering and Informatics*, pp. 888–892, May 2008, doi: 10.1109/BMEI.2008.275.
- [14] L. S. Jayashree, R. Lakshmi Devi, N. Papandrianos, and E. I. Papageorgiou, “Application of Fuzzy Cognitive Map for geospatial dengue outbreak risk prediction of tropical regions of Southern India,” *Int. Dec. Tech.*, vol. 12, no. 2, pp. 231–250, Jan. 2018, doi: 10.3233/IDT-180330.
- [15] S. G. K. Patro and K. K. Sahu, “Normalization: A Preprocessing Stage,” *Mar.* 19, 2015, arXiv: arXiv:1503.06462. doi: 10.48550/arXiv.1503.06462.
- [16] D. Berrar, “Cross-Validation,” 2018. doi: 10.1016/B978-0-12-809633-8.20349-X.
- [17] D. Wang, D. Tan, and L. Liu, “Particle swarm optimization algorithm: an overview,” *Soft Comput*, vol. 22, no. 2, pp. 387–408, Jan. 2018, doi: 10.1007/s00500-016-2474-6.
- [18] A. Lambora, K. Gupta, and K. Chopra, “Genetic Algorithm-A Literature Review,” in *2019 International Conference on Machine Learning, Big Data, Cloud and Parallel Computing (COMITCon)*, Oct. 2019, pp. 380–384. doi: 10.1109/COMITCon.2019.8862255.
- [19] R. R. Selvaraju, M. Cogswell, A. Das, R. Vedantam, D. Parikh, and D. Batra, “Grad-CAM: Visual Explanations from Deep Networks via Gradient-based Localization,” *Int J Comput Vis*, vol. 128, no. 2, pp. 336–359, Feb. 2020, doi: 10.1007/s11263-019-01228-7.
- [20] E. A. M. van Dis, J. Bollen, W. Zuidema, R. van Rooij, and C. L. Bockting, “ChatGPT: five priorities for research,” *Nature*, vol. 614, no. 7947, pp. 224–226, Feb. 2023, doi: 10.1038/d41586-023-00288-7.
- [21] “emeraldUTH · GitHub.” Accessed: Oct. 28, 2024. [Online]. Available: <https://github.com/emeraldUTH>